Neutrino and Nuclear Properties from Coherent Elastic Neutrino-Nucleus Scattering

Carlo Giunti

INFN, Torino, Italy

Colloquium at Roma Tre University, 8 June 2021

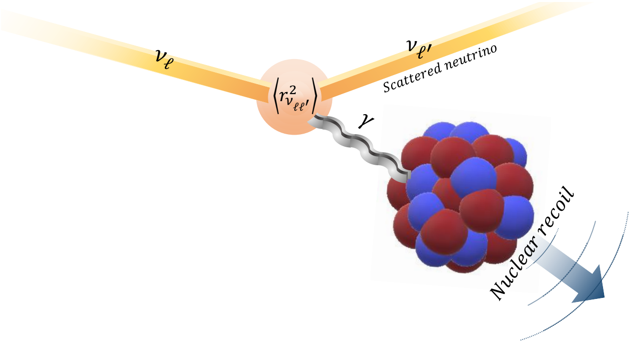

Coherent Elastic Neutrino-Nucleus Scattering

- CEνNS: pronounced “sevens”
- Weak Neutral-Current (NC) interaction:

$$\nu_\alpha + \mathcal{N}(A,Z) \to \nu_\alpha + \mathcal{N}(A,Z)$$

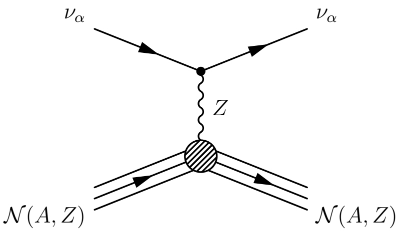

- The nucleus $\mathcal{N}(A,Z)$ recoils as a whole!
- So what? E allora? Embè?

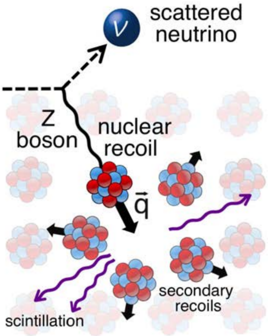

- Big cross section enhancement for heavy nuclei $\mathcal{N}(A, Z)$ with many nucleons N_i:
  - Incoherent scattering: $\sigma(\nu\mathcal{N}) \sim \sum_i |\mathcal{A}(\nu N_i)|^2 \propto A$
  - Coherent scattering: $\sigma(\nu\mathcal{N}) \sim \left|\sum_i \mathcal{A}(\nu N_i)\right|^2 \propto A^2$

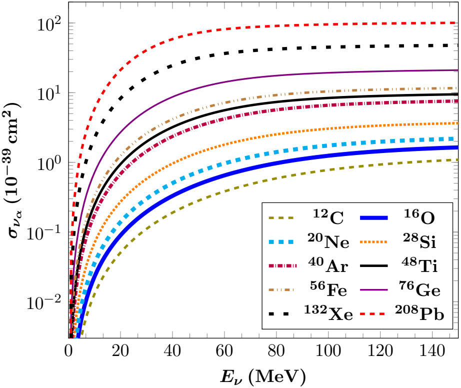

[Papoulias, Kosmas, Kuno, arXiv:1911.00916]

Neutrino-Nucleus Scattering

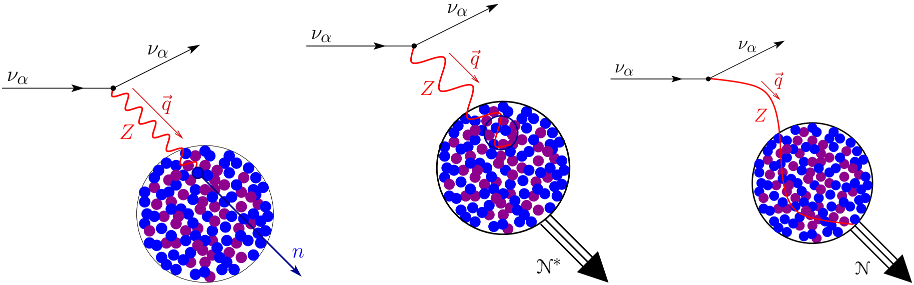

Inelastic Incoherent	Elastic Incoherent	Elastic Coherent
$\lambda_Z \ll R$	$\lambda_Z \lesssim R$	$\lambda_Z \gtrsim 2R$

$$\lambda_Z = 2\pi \frac{\hbar}{|\vec{q}|} \quad \Longrightarrow \quad \text{CE}\nu\text{NS for } |\vec{q}|\,R \lesssim \hbar$$

$$\boxed{|\vec{q}|\,R \lesssim 1} \quad \leftarrow \quad \text{Natural Units}$$

$$|\vec{q}|\,R \lesssim 1$$

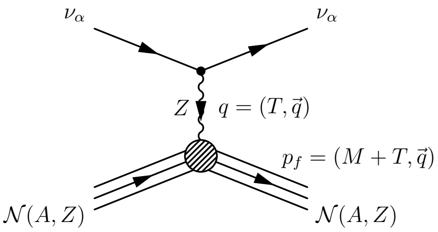

- Heavy target nucleus $\mathcal{N}(A, Z)$:

$$A \sim 100 \qquad M \sim 100\,\text{GeV}$$

$$R \approx 1.2\, A^{1/3}\,\text{fm} \approx 5\,\text{fm}$$

- CEνNS for $|\vec{q}| \lesssim 40\,\text{MeV}$

- Non-Relativistic nuclear recoil:

$$|\vec{q}| \simeq \sqrt{2\,M\,T} \qquad\qquad q^0 = T \quad \leftarrow \quad \text{Kinetic Energy}$$

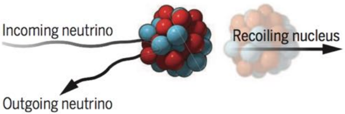

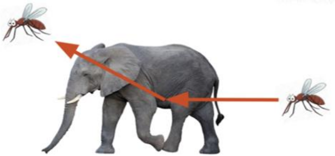

- Observable nuclear recoil kinetic energy:

$$T \simeq \frac{|\vec{q}|^2}{2\,M} \lesssim 10\,\text{keV} \quad \leftarrow \quad \text{Very Small!}$$

- CEνNS was predicted in 1974! [Freedman, PRD 9 (1974) 1389]

PHYSICAL REVIEW D VOLUME 9, NUMBER 5 1 MARCH 1974

Coherent effects of a weak neutral current

Daniel Z. Freedman†
National Accelerator Laboratory, Batavia, Illinois 60510
and Institute for Theoretical Physics, State University of New York, Stony Brook, New York 11790

(Received 15 October 1973; revised manuscript received 19 November 1973)

Our suggestion may be an act of hubris, because the inevitable constraints of interaction rate, resolution, and background pose grave experimental difficulties for elastic neutrino-nucleus scattering.

Experimentally the most conspicuous and most difficult feature of our process is that the only detectable reaction product is a recoil nucleus of low momentum. Ideally the apparatus should

- CEνNS was observed for the first time 43 years later, in 2017 by the COHERENT experiment at the Oak Ridge Spallation Neutron Source with CsI ($^{133}_{55}\mathrm{Cs}_{78}$, $^{127}_{53}\mathrm{I}_{74}$) and a threshold $T_{\mathrm{thr}} \simeq 5\,\mathrm{keV}$ [arXiv:1708.01294]

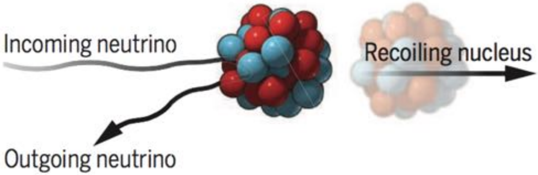

Maximum momentum transfer for $\vec{p}_{\nu_f} = -\vec{p}_{\nu_i}$

$$\vec{q} = \vec{p}_{\nu_i} - \vec{p}_{\nu_f} \Longrightarrow \underbrace{|\vec{q}|}_{\sqrt{2\,M\,T}} \leq 2\,|\vec{p}_{\nu_i}| = 2\,E_\nu$$

$$\boxed{T \leq \frac{2\,E_\nu^2}{M}}$$

Low-energy neutrinos are needed!

$$T \lesssim 10\,\text{keV} \quad \text{and} \quad M \sim 100\,\text{GeV} \quad \Longrightarrow \quad E_\nu \lesssim 30\,\text{MeV}$$

Natural sources of low-energy neutrinos

Supernova burst neutrinos

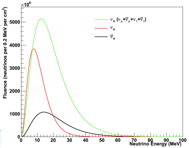

Every ~30 years in the Galaxy,~few 10's of sec burst, all flavors

Supernova relic neutrinos

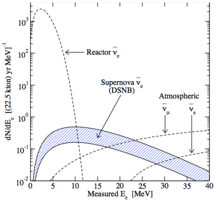

All flavors, low flux

Atmospheric neutrinos

Some component at low energy

Solar neutrinos

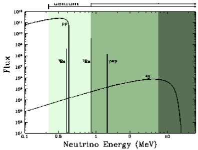

Most flux below 1 MeV

CEvNS eventually seen in DM expts

Geoneutrinos

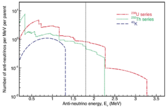

Very low energy

[Scholberg @ CNNP2017]

Artificial sources of low-energy neutrinos

Reactors

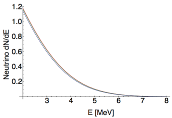

Low energy, but very high fluxes possible; ~continuous source, good bg rejection needed

Stopped pions
(decay at rest)

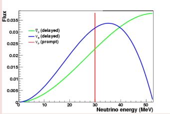

High energy, pulsed beam possible for good background rejection; possible neutron backgrounds

Radioactive sources
(electron capture)

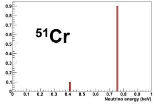

Portable; can get very short baseline, monochromatic

Low energy challenging

Beam-induced radioactive sources
(IsoDAR)

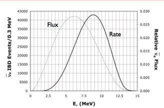

Relatively compact, higher energy than reactor; time structure not sharp

Does not exist yet

Low-energy beta beams

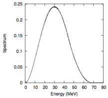

γ=10 boosted ^{18}Ne ν_e

Tunable energy, but not pulsed

Does not exist yet

[Scholberg @ CNNP2017]

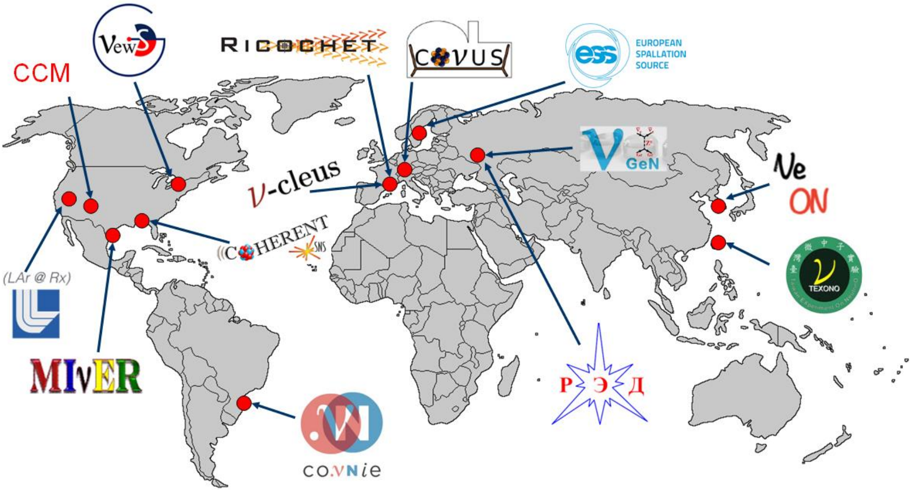

CEvNS search and study experiments around the world

[Konovalov @ Magnificent CEνNS 2020]

Reactor vs stopped-pion for CEvNS

Source	Flux/ ν's per s	Flavor	Energy	Pros	Cons
Reactor 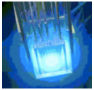	2e20 per GW	nuebar	few MeV	• huge flux	• lower xscn • require very low threshold • CW
Stopped pion 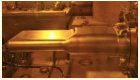	1e15	numu/ nue/ nuebar	0-50 MeV	• higher xscn • higher energy recoils • pulsed beam for bg rejection • multiple flavors	• lower flux • potential fast neutron in-time bg

[Scholberg @ CNNP2017]

Reactor CEvNS Experiments

Experiment	Technology	Location
CONUS	HPGe	Germany
Ricochet	Ge, Zn bolometers	France
CONNIE	Si CCDs	Brazil
RED	LXe dual phase	Russia
Nu-Cleus	Cryogenic $CaWO_4$, Al_2O_3 calorimeter array	Europe
MINER	Ge iZIP detectors	USA

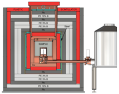

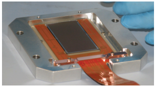
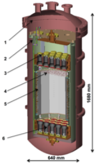
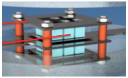


Novel low-background, low-threshold technologies

[Scholberg @ CNNP2017]

Stopped-Pion (πDAR) Neutrinos

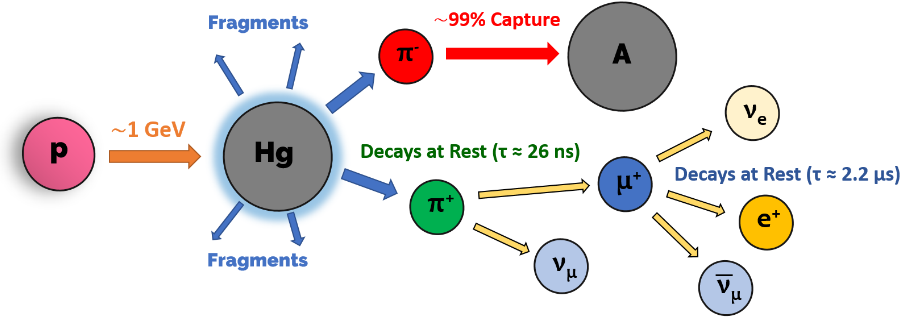

[M. Green @ Magnificent CEvNS 2019]

Stopped-Pion Neutrino Spectrum

- Prompt monochromatic ν_μ from stopped pion decays:

$$\pi^+ \to \mu^+ + \nu_\mu$$

$$\frac{dN_{\nu_\mu}}{dE_\nu} = \eta\,\delta\left(E_\nu - \frac{m_\pi^2 - m_\mu^2}{2m_\pi}\right)$$

- Delayed $\bar{\nu}_\mu$ and ν_e from the subsequent muon decays:

$$\mu^+ \to e^+ + \bar{\nu}_\mu + \nu_e$$

$$\frac{dN_{\nu_{\bar{\mu}}}}{dE_\nu} = \eta\,\frac{64E_\nu^2}{m_\mu^3}\left(\frac{3}{4} - \frac{E_\nu}{m_\mu}\right)$$

$$\frac{dN_{\nu_e}}{dE_\nu} = \eta\,\frac{192E_\nu^2}{m_\mu^3}\left(\frac{1}{2} - \frac{E_\nu}{m_\mu}\right)$$

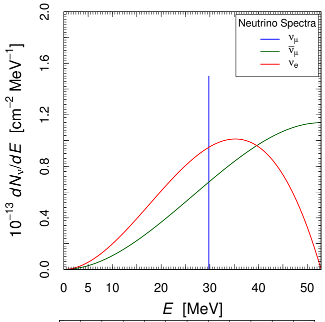

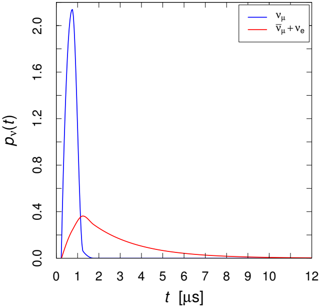

Stopped-Pion Neutrino Sources Worldwide

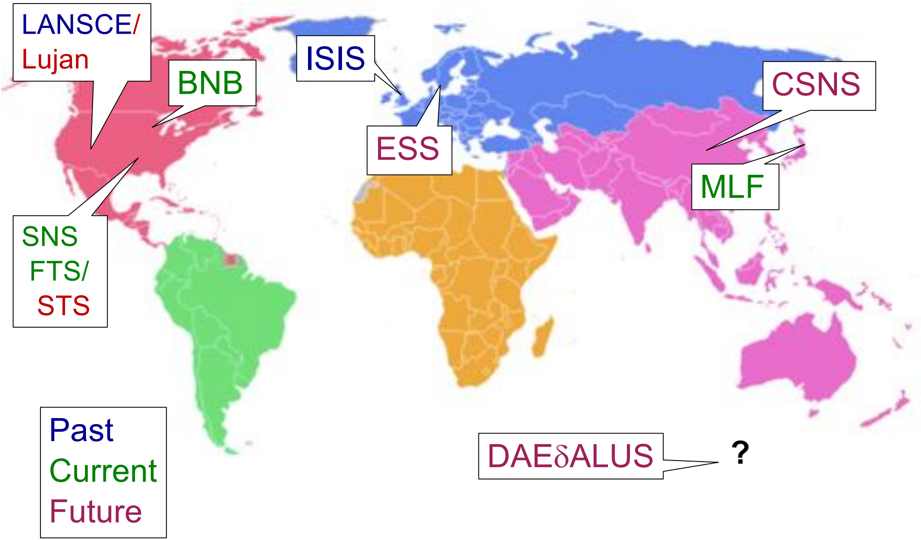

[Scholberg, GSSI Seminar 2020]

Comparison of pion decay-at-rest ν sources

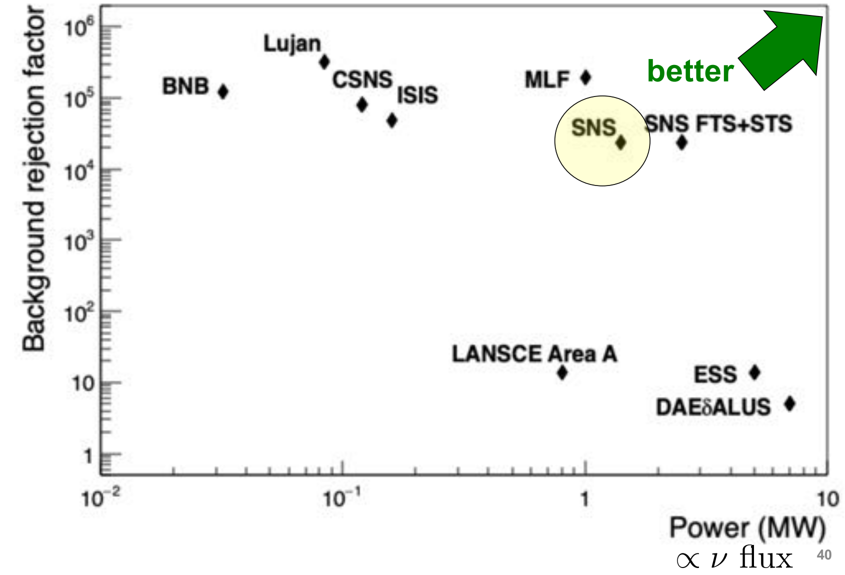

[Scholberg, GSSI Seminar 2020]

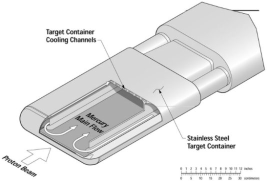

Proton beam energy: 0.9-1.3 GeV
Total power: 0.9-1.4 MW
Pulse duration: 380 ns FWHM
Repetition rate: 60 Hz
Liquid mercury target

The neutrinos are free!

27

[Scholberg @ CNNP2017]

Time structure of the SNS source

60 Hz *pulsed* source

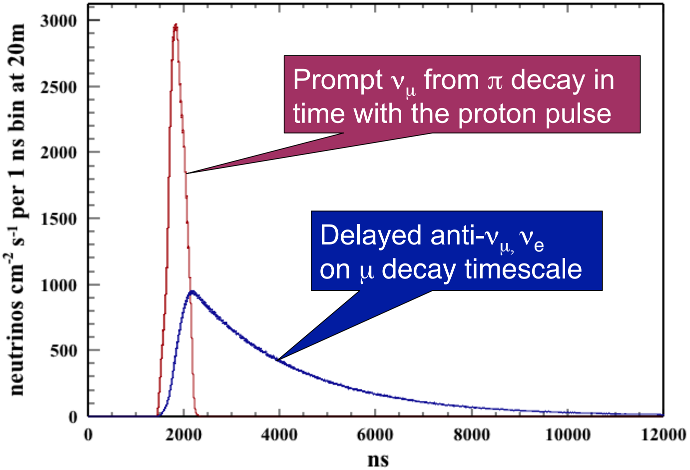

Background rejection factor ~few x 10^{-4}

[Scholberg @ CNNP2017]

The COHERENT Experiment

Oak Ridge Spallation Neutron Source

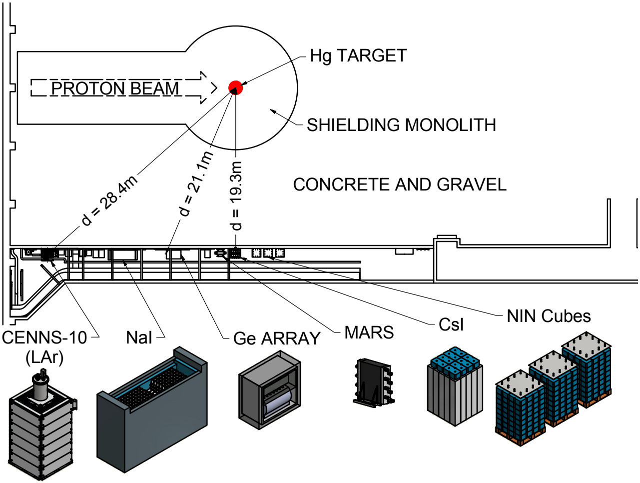

14.6 kg CsI
scintillating crystal

[COHERENT, arXiv:1803.09183]

COHERENT 2017: Cesium Iodide (CsI)

[arXiv:1708.01294]

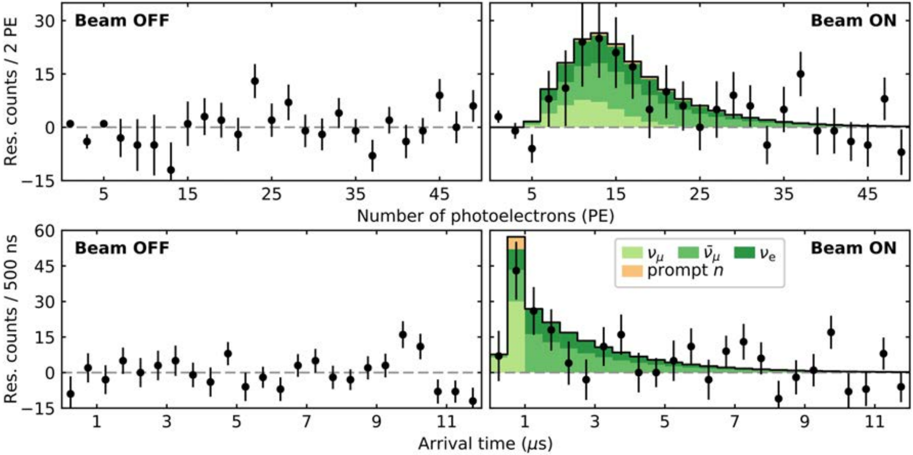

$^{133}_{55}Cs_{78}$ and $^{127}_{53}I_{74}$ $\leftarrow$ Heavy nuclei well suited for CEνNS

COHERENT 2020: Argon (Ar)

[arXiv:2003.10630]

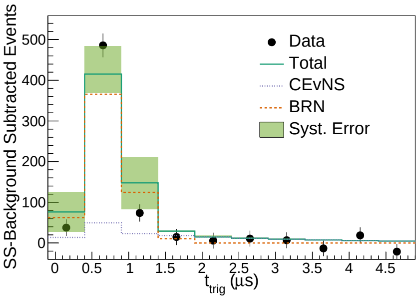

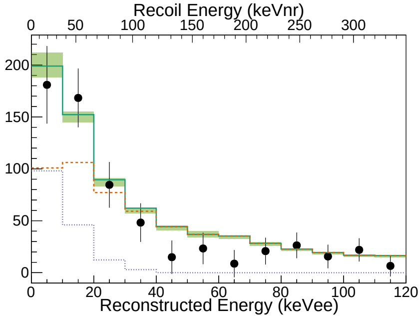

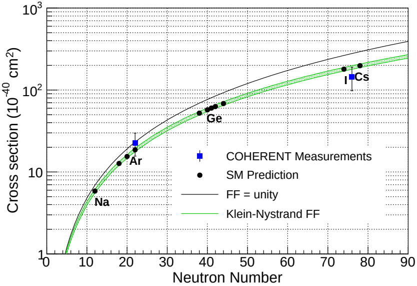

${}^{40}_{18}\mathrm{Ar}_{22}$ not so heavy

Verified theoretical $\sigma \propto N^2$

CEνNS Cross Section

$$\frac{d\sigma_{\nu\mathcal{N}}}{dT}(E_\nu, T) = \frac{G_F^2 M}{4\pi}\left(1 - \frac{MT}{2E_\nu^2}\right)\left[Q_W^{\mathcal{N}}(Q^2)\right]^2$$

- Weak charge of the nucleus $\mathcal{N}$:

$$Q_W^{\mathcal{N}}(Q^2) = g_V^n\, N_{\mathcal{N}}\, F_N^{\mathcal{N}}(|\vec{q}|^2) + g_V^p\, Z_{\mathcal{N}}\, F_Z^{\mathcal{N}}(|\vec{q}|^2)$$

$$g_V^n = -\frac{1}{2} \qquad g_V^p = \frac{1}{2} - 2\sin^2\vartheta_W(Q^2 \simeq 0) = 0.0227 \pm 0.0002$$

The neutron contribution is dominant! $\Longrightarrow$ $\dfrac{d\sigma_{\nu\mathcal{N}}}{dT} \underset{\sim}{\propto} N_{\mathcal{N}}^2$

- The form factors $F_N(|\vec{q}|^2)$ and $F_Z(|\vec{q}|^2)$ describe the loss of coherence for $|\vec{q}|R \gtrsim 1$.

[see: Bednyakov, Naumov, arXiv:1806.08768]

- In the COHERENT experiment neutrino-nucleus scattering is not completely coherent. For CsI:

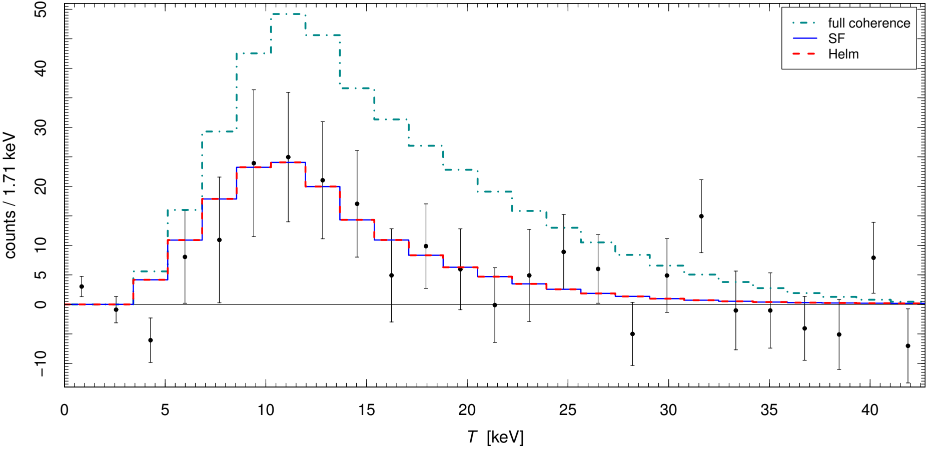

[Cadeddu, CG, Y.F. Li, Y.Y. Zhang, PRL 120 (2018) 072501, arXiv:1710.02730]

- Partial coherency gives information on the nuclear neutron form factor $F_N(|\vec{q}|^2)$, which is the Fourier transform of the neutron distribution in the nucleus.

Helm form factor: $F_N^{\text{Helm}}(|\vec{q}|^2) = 3\,\frac{j_1(|\vec{q}|R_0)}{|\vec{q}|R_0}\,e^{-|\vec{q}|^2 s^2/2}$

Spherical Bessel function of order one: $j_1(x) = \sin(x)/x^2 - \cos(x)/x$

Obtained from the convolution of a sphere with constant density with radius R_0 and a gaussian density with standard deviation s

Rms radius: $R^2 = \langle r^2 \rangle = \frac{3}{5}\,R_0^2 + 3s^2$ Surface thickness: $s \simeq 0.9\,\text{fm}$

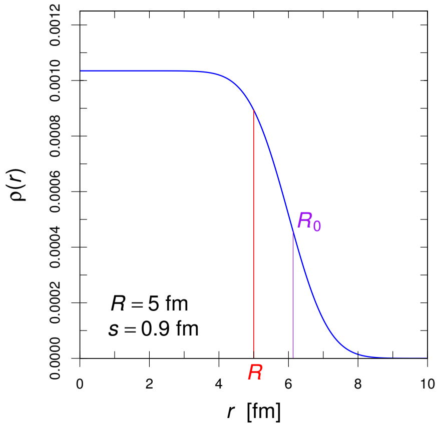

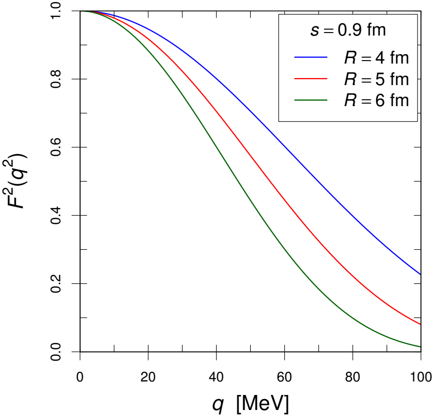

Helm form factor: $F_N^{\text{Helm}}(|\vec{q}|^2) = 3\,\frac{j_1(|\vec{q}|R_0)}{|\vec{q}|R_0}\,e^{-|\vec{q}|^2 s^2/2}$

Spherical Bessel function of order one: $j_1(x) = \sin(x)/x^2 - \cos(x)/x$

Obtained from the convolution of a sphere with constant density with radius R_0 and a gaussian density with standard deviation s

Rms radius: $R^2 = \langle r^2 \rangle = \frac{3}{5}\,R_0^2 + 3s^2$ Surface thickness: $s \simeq 0.9\,\text{fm}$

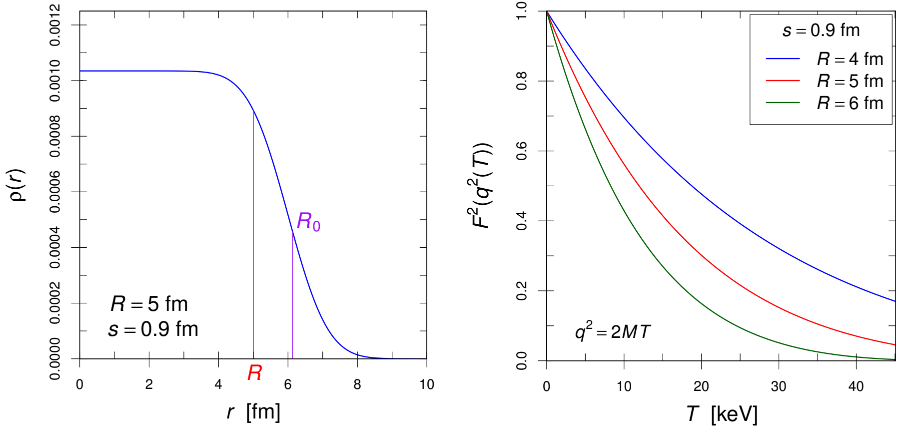

The Nuclear Proton and Neutron Distributions

- The nuclear proton distribution (charge density) is probed with electromagnetic interactions.
- Most sensitive are electron-nucleus elastic scattering and muonic atom spectroscopy.
- Hadron scattering experiments give information on the nuclear neutron distribution, but their interpretation depends on the model used to describe non-perturbative strong interactions.
- More reliable are neutral current weak interaction measurements.
  But they are more difficult.
- Before 2017 there was only one measurement of R_n with neutral-current weak interactions through parity-violating electron scattering:

$$R_n(^{208}\mathrm{Pb}) = 5.78^{+0.16}_{-0.18}\,\mathrm{fm}$$

[PREX, PRL 108 (2012) 112502]

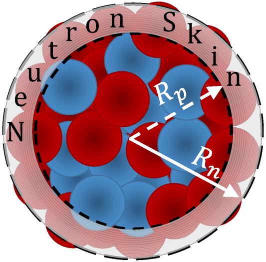

- The charge radii of ^{133}Cs and ^{127}I have been determined with muonic atom spectroscopy: [Angeli, Marinova, ADNDT 99 (2013) 69]

$$R_c(^{133}\text{Cs}) = 4.8041 \pm 0.0046\,\text{fm}$$

$$R_c(^{127}\text{I}) = 4.7500 \pm 0.0081\,\text{fm}$$

- Radius of the proton distribution: $R_p^2 = R_c^2 - \frac{N}{Z}\langle r_n^2 \rangle_c$

[Ong, Berengut, Flambaum, arXiv:1006.5508; Horowitz et al, arXiv:1202.1468]

- Squared charge radius of the neutron:

$$\langle r_n^2 \rangle_c = -0.1161 \pm 0.0022\,\text{fm}^2$$ [PDG 2018]

- Radii of the proton distributions of ^{133}Cs and ^{127}I:

$$R_p(^{133}\text{Cs}) = 4.821 \pm 0.005\,\text{fm}$$

$$R_p(^{127}\text{I}) = 4.766 \pm 0.008\,\text{fm}$$

- Fit of the 2017 COHERENT CsI data to get $R_n(^{133}\mathrm{Cs}) \simeq R_n(^{127}\mathrm{I})$:

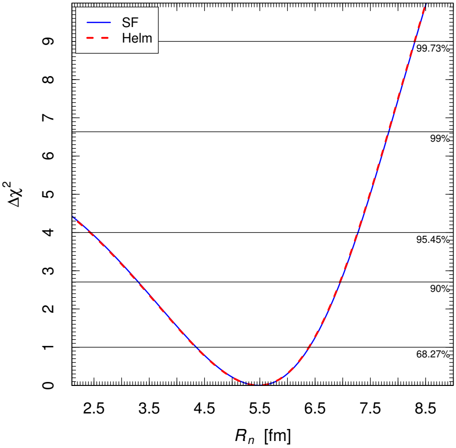

First determination of R_n with neutrino-nucleus scattering:

$$R_n(\mathrm{CsI}) = 5.5^{+0.9}_{-1.1}\ \mathrm{fm}$$

[Cadeddu, Giunti, Li, Zhang, arXiv:1710.02730]

- With new 2020 COHERENT CsI data: [Pershey @ Magnificent CEνNS 2020]

$$R_n(\mathrm{CsI}) = 5.55 \pm 0.44\ \mathrm{fm}$$

[Cadeddu et al, arXiv:2102.06153]

$$R_n(\mathrm{CsI}) = 5.55 \pm 0.44\,\mathrm{fm}$$

- The uncertainty is large, but it can be improved in future.
- Predictions of nuclear models: $R_n(\mathrm{CsI}) \approx 4.9 - 5.1\,\mathrm{fm}$
- A large R_n has important implications for:
  - Nuclear physics: a larger pressure of neutrons
  - Astrophysics: a larger size of neutron stars

BSM Neutrino Interactions in CEνNS

Standard Model NC

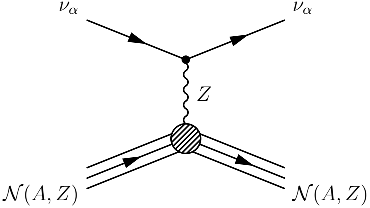

+

Electromagnetic Interactions

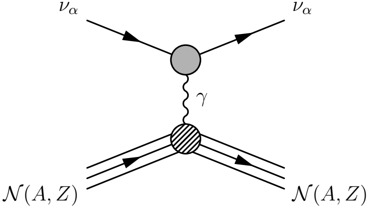

+

BSM Vector Mediator

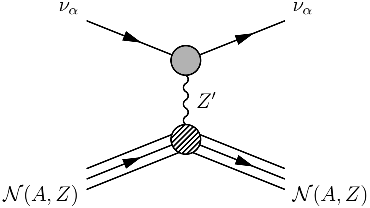

+

BSM Scalar Mediator

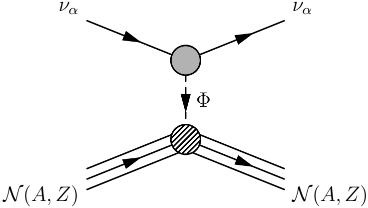

Neutrino Electromagnetic Interactions

- Effective Hamiltonian: $\mathcal{H}_{\text{em}}^{(\nu)}(x) = j_{\mu}^{(\nu)}(x) A^{\mu}(x) = \sum_{k,j=1} \overline{\nu_k}(x) \Lambda_{\mu}^{kj} \nu_j(x) A^{\mu}(x)$

- Effective electromagnetic vertex:

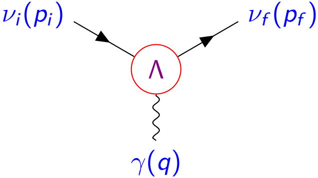

$$\langle \nu_f(p_f) | j_{\mu}^{(\nu)}(0) | \nu_i(p_i) \rangle = \overline{u_f}(p_f) \Lambda_{\mu}^{fi}(q) u_i(p_i)$$

$$q = p_i - p_f$$

- Vertex function:

$$\Lambda_{\mu}(q) = \left(\gamma_{\mu} - q_{\mu} \not{q}/q^2\right) \left[F_Q(q^2) + F_A(q^2) q^2 \gamma_5\right] - i \sigma_{\mu\nu} q^{\nu} \left[F_M(q^2) + i F_E(q^2) \gamma_5\right]$$

Lorentz-invariant form factors: charge (F_Q), anapole (F_A), magnetic (F_M), electric (F_E)

$q^2 = 0 \implies$ charge → q, anapole → a, magnetic → μ, electric → ε

helicity-conserving: q, a

helicity-flipping: μ, ε

Electromagnetic Vertex Function

$$\Lambda_\mu(q) = \left(\gamma_\mu - q_\mu \not{q}/q^2\right)\left[F_Q(q^2) + F_A(q^2) q^2 \gamma_5\right] - i\sigma_{\mu\nu} q^\nu \left[F_M(q^2) + i F_E(q^2)\gamma_5\right]$$

Lorentz-invariant form factors:	charge	anapole	magnetic	electric
$q^2 = 0 \implies$	q	a	μ	ε

- Hermitian form factors: $F_Q = F_Q^\dagger$, $F_A = F_A^\dagger$, $F_M = F_M^\dagger$, $F_E = F_E^\dagger$
- Majorana neutrinos: $F_Q = -F_Q^T$, $F_A = F_A^T$, $F_M = -F_M^T$, $F_E = -F_E^T$

no diagonal charges and electric and magnetic moments in the mass basis

- For left-handed ultrarelativistic neutrinos $\gamma_5 \to -1 \Rightarrow$ The phenomenology of the charge and anapole are similar and the phenomenology of the magnetic and electric moments are similar.
- For ultrarelativistic neutrinos the charge and anapole terms conserve helicity, whereas the magnetic and electric terms invert helicity.

Neutrino Charge Radius

- In the Standard Model neutrinos are neutral and there are no electromagnetic interactions at the tree-level.

- Radiative corrections generate an effective electromagnetic interaction vertex

$$\Lambda_\mu(q) = \left(\gamma_\mu - q_\mu \not{q}/q^2\right) F(q^2)$$

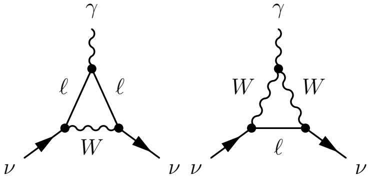

- $F(q^2) = \cancel{F(0)} + q^2 \left. \frac{dF(q^2)}{dq^2} \right|_{q^2=0} + \ldots = q^2 \frac{\langle r^2 \rangle}{6} + \ldots$

- In the Standard Model: [Bernabeu et al, PRD 62 (2000) 113012, NPB 680 (2004) 450]

$$\langle r^2_{\nu_\ell} \rangle_{\text{SM}} = -\frac{G_{\text{F}}}{2\sqrt{2}\pi^2} \left[3 - 2 \log \left(\frac{m_\ell^2}{m_W^2} \right) \right]$$

$$\langle r^2_{\nu_e} \rangle_{\text{SM}} = -8.2 \times 10^{-33}\,\text{cm}^2$$
$$\langle r^2_{\nu_\mu} \rangle_{\text{SM}} = -4.8 \times 10^{-33}\,\text{cm}^2$$
$$\langle r^2_{\nu_\tau} \rangle_{\text{SM}} = -3.0 \times 10^{-33}\,\text{cm}^2$$

Experimental Bounds

Method	Experiment	Limit [cm^2]	CL	Year
Reactor $\bar{\nu}_e\, e^-$	Krasnoyarsk	$\lvert\langle r^2_{\nu_e}\rangle\rvert < 7.3 \times 10^{-32}$	90%	1992
	TEXONO	$-4.2 \times 10^{-32} < \langle r^2_{\nu_e}\rangle < 6.6 \times 10^{-32}$	90%	2009
Accelerator $\nu_e\, e^-$	LAMPF	$-7.12 \times 10^{-32} < \langle r^2_{\nu_e}\rangle < 10.88 \times 10^{-32}$	90%	1992
	LSND	$-5.94 \times 10^{-32} < \langle r^2_{\nu_e}\rangle < 8.28 \times 10^{-32}$	90%	2001
Accelerator $\nu_\mu\, e^-$	BNL-E734	$-5.7 \times 10^{-32} < \langle r^2_{\nu_\mu}\rangle < 1.1 \times 10^{-32}$	90%	1990
	CHARM-II	$\lvert\langle r^2_{\nu_\mu}\rangle\rvert < 1.2 \times 10^{-32}$	90%	1994

[see the review Giunti, Studenikin, arXiv:1403.6344

and the update in Cadeddu, Giunti, Kouzakov, Y.F. Li, Studenikin, Y.Y. Zhang, arXiv:1810.05606]

- Neutrino charge radii contributions to ν_ℓ–$\mathcal{N}$ CEνNS:

$$\frac{d\sigma_{\nu_\ell\text{-}\mathcal{N}}}{dT}(E_\nu, T) = \frac{G_F^2 M}{\pi}\left(1 - \frac{MT}{2E_\nu^2}\right)\left\{\left[\underbrace{-\frac{1}{2}}_{g_V^n} N F_N(|\vec{q}|^2) + \left(\underbrace{\frac{1}{2} - 2\sin^2\vartheta_W}_{g_V^p \simeq 0.023} - \frac{2}{3} m_W^2 \sin^2\vartheta_W \langle r_{\nu_{\ell\ell}}^2\rangle\right) Z F_Z(|\vec{q}|^2)\right]^2 + \frac{4}{9} m_W^4 \sin^4\vartheta_W Z^2 F_Z^2(|\vec{q}|^2) \sum_{\ell' \neq \ell} |\langle r_{\nu_{\ell'\ell}}^2\rangle|^2\right\}$$

- In the Standard Model there are only diagonal charge radii $\langle r_{\nu_\ell}^2\rangle \equiv \langle r_{\nu_{\ell\ell}}^2\rangle$ because lepton numbers are conserved.

- Diagonal charge radii generate the coherent shifts

$$\sin^2\vartheta_W \to \sin^2\vartheta_W\left(1 + \frac{1}{3} m_W^2 \langle r_{\nu_\ell}^2\rangle\right) \quad \Longleftrightarrow \quad \nu_\ell + \mathcal{N} \to \nu_\ell + \mathcal{N}$$

- Transition charge radii generate the incoherent contribution

$$\frac{4}{9} m_W^4 \sin^4\vartheta_W Z^2 F_Z^2(|\vec{q}|^2) \sum_{\ell' \neq \ell} |\langle r_{\nu_{\ell'\ell}}^2\rangle|^2 \quad \Longleftrightarrow \quad \nu_\ell + \mathcal{N} \to \sum_{\ell' \neq \ell} \nu_{\ell' \neq \ell} + \mathcal{N}$$

[Kouzakov, Studenikin, PRD 95 (2017) 055013, arXiv:1703.00401]

COHERENT constraints on neutrino charge radii

[Cadeddu et al, arXiv:2005.01645]

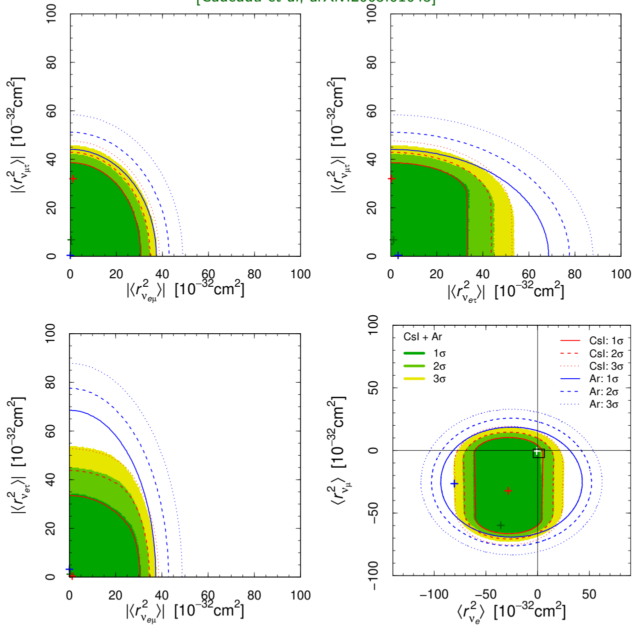

Neutrino Electric Charges

- Neutrinos can be millicharged particles in theories beyond the Standard Model.

- Neutrino charge contributions to ν_ℓ–$\mathcal{N}$ CEνNS:

$$\frac{d\sigma_{\nu_\ell\text{-}\mathcal{N}}}{dT}(E_\nu, T) = \frac{G_F^2 M}{\pi}\left(1 - \frac{MT}{2E_\nu^2}\right)\left\{\left[\underbrace{-\frac{1}{2}}_{g_V^n} N F_N(|\vec{q}|^2) + \left(\underbrace{\frac{1}{2} - 2\sin^2\vartheta_W}_{g_V^p \simeq 0.023} + \frac{2m_W^2 \sin^2\vartheta_W}{MT}\, q_{\nu_{\ell\ell}}\right) Z F_Z(|\vec{q}|^2)\right]^2 + \frac{4m_W^4 \sin^4\vartheta_W}{M^2 T^2}\, Z^2 F_Z^2(|\vec{q}|^2) \sum_{\ell' \neq \ell} |q_{\nu_{\ell\ell'}}|^2\right\}$$

- $q_{\bar{\nu}_{\ell\ell'}} = -q_{\nu_{\ell\ell'}}$, but also $g_V^{p,n}(\bar{\nu}) = -g_V^{p,n}(\nu)$.

Approximate limits on neutrino millicharges

Limit	Method	Reference
$\lvert q_{\nu_e}\rvert \lesssim 3 \times 10^{-21}\, e$	Neutrality of matter	Raffelt (1999)
$\lvert q_{\nu_e}\rvert \lesssim 3.7 \times 10^{-12}\, e$	Nuclear reactor	Gninenko et al, (2006)
$\lvert q_{\nu_e}\rvert \lesssim 1.5 \times 10^{-12}\, e$	Nuclear reactor	Studenikin (2013)
$\lvert q_{\nu_\tau}\rvert \lesssim 3 \times 10^{-4}\, e$	SLAC e^- beam dump	Davidson et al, (1991)
$\lvert q_{\nu_\tau}\rvert \lesssim 4 \times 10^{-4}\, e$	BEBC beam dump	Babu et al, (1993)
$\lvert q_{\nu}\rvert \lesssim 6 \times 10^{-14}\, e$	Solar cooling (plasmon decay)	Raffelt (1999)
$\lvert q_{\nu}\rvert \lesssim 2 \times 10^{-14}\, e$	Red giant cooling (plasmon decay)	Raffelt (1999)

Neutrality of matter

- From electric charge conservation in neutron beta decay $(n \to p + e^- + \bar{\nu}_e)$

$$q_{\nu_e} = q_n - (q_p + q_e) = \frac{A}{Z}(q_n - q_{\text{mat}}) \quad \text{with} \quad q_{\text{mat}} = \frac{Z(q_p + q_e) + N q_n}{A}$$

- $q_{\text{mat}} = (-0.1 \pm 1.1) \times 10^{-21}\, e$ with SF_6, which has $A = 146.06$ and $Z = 70$

[Bressi, et al., PRA 83 (2011) 052101, arXiv:1102.2766]

- $q_n = (-0.4 \pm 1.1) \times 10^{-21}\, e$ [Baumann, Kalus, Gahler, Mampe, PRD 37 (1988) 3107]

- $q_{\nu_e} = (-0.6 \pm 3.2) \times 10^{-21}\, e$ [Giunti, Studenikin, arXiv:1403.6344]

COHERENT constraints on neutrino millicharges

[Cadeddu et al, arXiv:2005.01645]

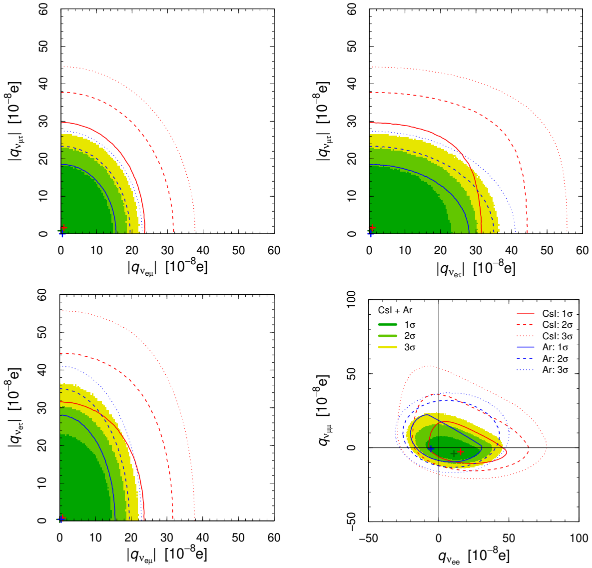

- The bounds on the charges involving the electron neutrino flavor
  $q_{\nu_{ee}}$ $q_{\nu_{e\mu}}$ $q_{\nu_{e\tau}}$
  are not competitive with respect to those obtained in reactor neutrino experiments, that are at the level of $10^{-12}\,e$ in neutrino-electron elastic scattering experiments.
- The bounds on
  $q_{\nu_{\mu\mu}}$ $q_{\nu_{\mu\tau}}$
  are the first ones obtained from laboratory data.

Neutrino Magnetic and Electric Moments

- Extended Standard Model with right-handed neutrinos and $\Delta L = 0$:

$$\mu_{kk}^{\text{D}} \simeq 3.2 \times 10^{-19} \mu_{\text{B}} \left(\frac{m_k}{\text{eV}} \right) \qquad \varepsilon_{kk}^{\text{D}} = 0$$

$$\left. \begin{matrix} \mu_{kj}^{\text{D}} \\ i\varepsilon_{kj}^{\text{D}} \end{matrix} \right\} \simeq -3.9 \times 10^{-23} \mu_{\text{B}} \left(\frac{m_k \pm m_j}{\text{eV}} \right) \sum_{\ell=e,\mu,\tau} U_{\ell k}^{*} U_{\ell j} \left(\frac{m_\ell}{m_\tau} \right)^2$$

off-diagonal moments are GIM-suppressed

[Fujikawa, Shrock, PRL 45 (1980) 963; Pal, Wolfenstein, PRD 25 (1982) 766; Shrock, NPB 206 (1982) 359; Dvornikov, Studenikin, PRD 69 (2004) 073001, JETP 99 (2004) 254]

- Extended Standard Model with Majorana neutrinos ($|\Delta L| = 2$):

$$\mu_{kj}^{\text{M}} \simeq -7.8 \times 10^{-23} \mu_{\text{B}} \, i \, (m_k + m_j) \sum_{\ell=e,\mu,\tau} \text{Im}\left[U_{\ell k}^{*} U_{\ell j} \right] \frac{m_\ell^2}{m_W^2}$$

$$\varepsilon_{kj}^{\text{M}} \simeq 7.8 \times 10^{-23} \mu_{\text{B}} \, i \, (m_k - m_j) \sum_{\ell=e,\mu,\tau} \text{Re}\left[U_{\ell k}^{*} U_{\ell j} \right] \frac{m_\ell^2}{m_W^2}$$

[Shrock, NPB 206 (1982) 359]

GIM-suppressed, but additional model-dependent contributions of the scalar sector can enhance the Majorana transition dipole moments

[Pal, Wolfenstein, PRD 25 (1982) 766; Barr, Freire, Zee, PRL 65 (1990) 2626; Pal, PRD 44 (1991) 2261]

$$\left(\frac{d\sigma_{\nu e^-}}{dT_e}\right)_{\text{mag}} = \frac{\pi\alpha^2}{m_e^2}\left(\frac{1}{T_e} - \frac{1}{E_\nu}\right)\left(\frac{\mu_\nu}{\mu_{\text{B}}}\right)^2$$

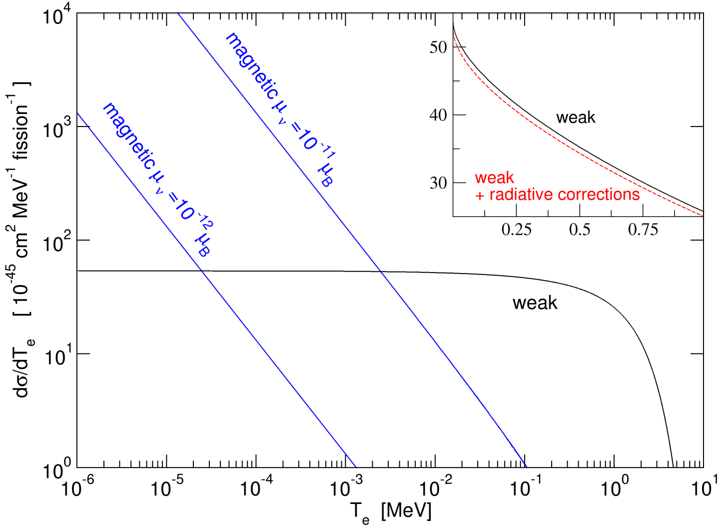

Method	Experiment	Limit $[\mu_B]$	CL	Year
Reactor $\bar{\nu}_e\, e^-$	Krasnoyarsk	$\mu_{\nu_e} < 2.4 \times 10^{-10}$	90%	1992
	Rovno	$\mu_{\nu_e} < 1.9 \times 10^{-10}$	95%	1993
	MUNU	$\mu_{\nu_e} < 9 \times 10^{-11}$	90%	2005
	TEXONO	$\mu_{\nu_e} < 7.4 \times 10^{-11}$	90%	2006
	GEMMA	$\mu_{\nu_e} < 2.9 \times 10^{-11}$	90%	2012
Accelerator $\nu_e\, e^-$	LAMPF	$\mu_{\nu_e} < 1.1 \times 10^{-9}$	90%	1992
Accelerator $(\nu_\mu, \bar{\nu}_\mu)\, e^-$	BNL-E734	$\mu_{\nu_\mu} < 8.5 \times 10^{-10}$	90%	1990
	LAMPF	$\mu_{\nu_\mu} < 7.4 \times 10^{-10}$	90%	1992
	LSND	$\mu_{\nu_\mu} < 6.8 \times 10^{-10}$	90%	2001
Accelerator $(\nu_\tau, \bar{\nu}_\tau)\, e^-$	DONUT	$\mu_{\nu_\tau} < 3.9 \times 10^{-7}$	90%	2001
Solar $\nu_e\, e^-$	Super-Kamiokande	$\mu_S(E_\nu \gtrsim 5\,\text{MeV}) < 1.1 \times 10^{-10}$	90%	2004
	Borexino	$\mu_S(E_\nu \lesssim 1\,\text{MeV}) < 2.8 \times 10^{-11}$	90%	2017

[see the review Giunti, Studenikin, arXiv:1403.6344]

- Gap of about 8 orders of magnitude between the experimental limits and the $\lesssim 10^{-19}\,\mu_B$ prediction of the minimal Standard Model extensions.
- $\mu_\nu \gg 10^{-19}\,\mu_B$ discovery $\Rightarrow$ non-minimal new physics beyond the SM.
- Neutrino spin-flavor precession in a magnetic field

[Lim, Marciano, PRD 37 (1988) 1368; Akhmedov, PLB 213 (1988) 64]

- Neutrino magnetic (and electric) moment contributions to CEνNS $\nu_\ell + \mathcal{N} \to \sum_{\ell'} \nu_{\ell'} + \mathcal{N}$:

$$\frac{d\sigma_{\nu_\ell\text{-}\mathcal{N}}}{dT}(E_\nu, T) = \frac{G_F^2 M}{\pi} \left(1 - \frac{MT}{2E_\nu^2}\right) \left[g_V^n N F_N(|\vec{q}|^2) + g_V^p Z F_Z(|\vec{q}|^2)\right]^2 + \frac{\pi\alpha^2}{m_e^2} \left(\frac{1}{T} - \frac{1}{E_\nu}\right) Z^2 F_Z^2(|\vec{q}|^2) \sum_{\ell' \neq \ell} \frac{|\mu_{\ell\ell'}|^2}{\mu_B^2}$$

- The magnetic moment interaction adds incoherently to the weak interaction because it flips helicity.

- The m_e is due to the definition of the Bohr magneton: $\mu_B = e/2m_e$.

COHERENT constraints on ν magnetic moments

[Cadeddu et al, arXiv:2005.01645]

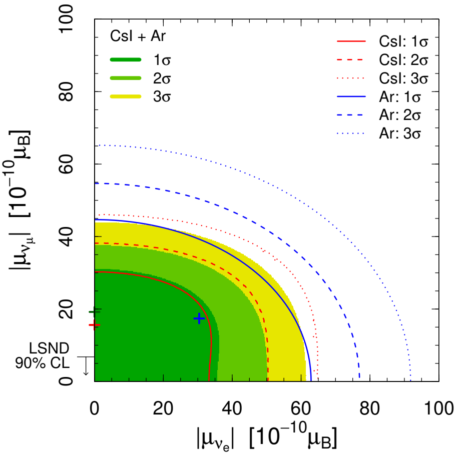

- The sensitivity to $|\mu_{\nu_e}|$ is not competitive with that of reactor experiments:

$$|\mu_{\nu_e}| < 2.9 \times 10^{-11}\,\mu_B \quad (90\%\ \mathrm{CL})$$

[GEMMA, AHEP 2012 (2012) 350150]

- The constraint on $|\mu_{\nu_\mu}|$ is not too far from the best current laboratory limit:

$$|\mu_{\nu_\mu}| < 6.8 \times 10^{-10}\,\mu_B \quad (90\%\ \mathrm{CL})$$

[LSND, PRD 63 (2001) 112001]

Conclusions

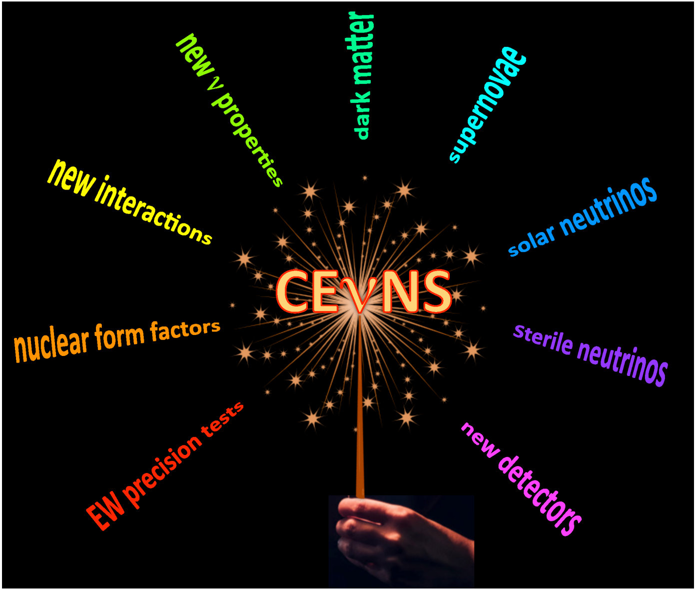

[E. Lisi, Neutrino 2018]